Published in final edited form as:
J Neuropathol Exp Neurol. 2012 April ; 71(4): 312–329. doi:10.1097/NEN.0b013e31824d9882.

Somatostatin and Neuropeptide Y Neurons Undergo Different Plasticity in Parahippocampal Regions in Kainic Acid–Induced Epilepsy

Meinrad Drexel, PhD, **Elke Kirchmair, BMA**, **Anna Wieselthaler-Hölzl, BMA**, **Adrian Patrick Preidt, Mag**, and **Günther Sperk, PhD**
Department of Pharmacology, Innsbruck Medical University, Innsbruck, Austria

Abstract

Parahippocampal brain areas including the subiculum, presubiculum and parasubiculum, and entorhinal cortex give rise to major input and output neurons of the hippocampus and exert increased excitability in animal models and human temporal lobe epilepsy. Using immunohistochemistry and in situ hybridization for somatostatin and neuropeptide Y, we investigated plastic morphologic and neurochemical changes in parahippocampal neurons in the kainic acid (KA) model of temporal lobe epilepsy. Although constitutively contained in similar subclasses of γ-aminobutyric acid (GABA)-ergic neurons, both neuropeptide systems undergo distinctly different changes in their expression. Somatostatin messenger RNA (mRNA) is rapidly but transiently expressed de novo in pyramidal neurons of the subiculum and entorhinal cortex 24 hours after KA. Surviving somatostatin interneurons display increased mRNA levels at late intervals (3 months) after KA and increased labeling of their terminals in the outer molecular layer of the subiculum; the labeling correlates with the number of spontaneous seizures, suggesting that the seizures may trigger somatostatin expression. In contrast, neuropeptide Y mRNA is consistently expressed in principal neurons of the proximal subiculum and the lateral entorhinal cortex and labeling for the peptide persistently increased in virtually all major excitatory pathways of the hippocampal formation. The pronounced plastic changes differentially involving both neuropeptide systems indicate marked rearrangement of parahippocampal areas, presumably aiming at endogenous seizure protection. Their receptors may be targets for anticonvulsive drug therapy.

Keywords

Entorhinal cortex; Epileptogenesis; Kainic acid; Neuropeptides; Status epilepticus; Subiculum; Temporal lobe epilepsy

INTRODUCTION

Epileptic seizures induce considerable morphologic and chemical plasticity in the hippocampal formation. Notably, dentate granule cells exert altered expression of a large number of functionally important proteins (1–5), and granule cell axons (so-called mossy fibers) show prominent sprouting to the inner molecular layer of the dentate gyrus where they presumably substitute for a loss of innervation by associational-commissural fibers (6–

Send correspondence and reprint requests to: Günther Sperk, PhD, Department of Pharmacology, Innsbruck Medical University, Peter-Mayr-Str. 1a, 6020 Innsbruck, Austria; guenther.sperk@i-med.ac.at.

8). Sprouting of Schaffer collaterals (axons of CA3 pyramidal neurons) to hippocampal sector CA1, the subiculum, the presubiculum and parasubiculum, and the entorhinal cortex (EC) has also been reported in kainic acid (KA)–induced epilepsy in the rat (9). Sprouting of CA1 pyramidal cell axons has been demonstrated in different animal models of temporal lobe epilepsy (TLE) and in human TLE (10–14). Target areas of sprouted CA1 pyramidal cell axons include not only all layers of sector CA1 but also sector CA3, the subiculum, and the alveus. Axonal sprouting, however, also involves γ-aminobutyric acid (GABA)-ergic interneurons. In human TLE, sprouting of calretinin (CR)-, neuropeptide Y (NPY)–, and somatostatin (SOM)-labeled fibers have been observed in the dentate gyrus, in the hippocampus proper, and in the subiculum (15–18).

Conspicuous overexpression of neuropeptides such as SOM and NPY in interneurons in the dentate gyrus and the hippocampus proper highlights striking neurochemical plasticity in epilepsy (1, 19–23). In addition to interneurons, NPY is prominently expressed in granule cells/mossy fibers in rat epilepsy models. At the same time, the expression of Y2 receptors is increased in mossy fibers of epileptic animals and in human TLE (17, 24, 25). By activating Y2 receptors, NPY inhibits glutamate release and exerts anticonvulsive actions (26–30). Thus, upregulation of NPY and of Y2 receptors may contribute to endogenous anticonvulsive mechanisms, and Y2 receptors may be targets for novel therapies for epilepsy (31). Similarly, SOM has been proposed to have an anticonvulsive role by activating sst2 receptors (32, 33). Thus, altered expression of neuropeptides may strongly influence the outcome of seizures.

Parahippocampal brain areas such as the subiculum and EC intimately interact with the hippocampal formation. They represent major output and input areas of the hippocampus, respectively, and may be crucially involved in the generation of epileptic activity, both in animal models and in human TLE (34–36). In human TLE, Layers II and III of the EC are severely affected by neurodegeneration (37), whereas the subiculum is surprisingly preserved in TLE and in patients with severe Ammon horn sclerosis (17, 38). In the KA and pilocarpine models of TLE, the proximal subiculum and Layer III of the medial EC undergo marked neurodegeneration including that of parvalbumin-positive neurons (35, 39, 40); cell losses in the distal subiculum, in EC Layer II and in the presubiculum, are less prominent (39) (unpublished observations). On the other hand, dense sprouting of GABA/NPY-ergic neurons has been demonstrated in the subiculum in human TLE (17) but not yet reported for the rat.

Because there is sparse information available on changes in neuropeptide systems of parahippocampal areas in epilepsy, we investigated morphologic and neurochemical plasticity of the SOM and NPY systems in parahippocampal brain areas, including the subiculum, presubiculum, parasubiculum, and EC in the KA model of TLE using immunohistochemistry and in situ hybridization (ISH).

MATERIALS AND METHODS

Rats

Male Sprague-Dawley rats (210–260 g; Forschungsinstitut für Versuchstierzucht, Himberg, Austria) were used for the study. The rats had free access to food and water and were housed at a temperature of 22 to 23°C, relative humidity of 50% to 60%, and a 12-hour light/dark cycle. All animal experiments were conducted according to national guidelines and European Community laws. They were approved by the Committee for Animal Protection of the Austrian Ministry of Science. All care was taken to minimize suffering of the rats.

KA Injection and Evaluation of Behavior

In total, 97 rats were injected intraperitoneally (i.p.) with 10 mg/kg KA (Ascent Scientific, Ltd, North Somerset, UK), dissolved in 0.9% NaCl at a concentration of 5 mg/ml and adjusted to pH 7.0. Seizure behavior was monitored for at least 3 hours and rated using a 5-stage rating system as previously described (41). Rats without any obvious behavioral changes were scored as stage 0; rats exhibiting “wet dog shakes” only were scored as stage 1; rats with chewing, head bobbing, and forelimb clonus were scored as stage 2; rats with generalized seizures and rearing were scored as stage 3; rats with generalized seizures, rearing, and falling (loss of postural tone) were scored as stage 4; and rats that died during status epilepticus (SE) were scored as stage 5. To reduce mortality and severity of the neuropathologic outcome, rats were treated with diazepam (10 mg/kg i.p., Gewacalm; Nycomed Austria GmbH, Linz, Austria) 2 hours after the first generalized seizure. Four rats developed stage 2 seizures, 51 rats developed stage 3, and 27 rats developed stage 4 seizures. Four rats did not respond, and 11 rats died. All rats with stage 3 and 4 were included in the study and were killed after different intervals (see tissue preparation).

Video-Assisted Telemetric EEG Recording

In 37 of the rats with seizures, video-assisted EEG recordings were performed for up to 3 months. A biopotential transmitter (TA10EA-F20; Data Sciences International, Arden Hills, MN) was placed in a subcutaneous pocket at the back of the rats and the transmitter leads were secured to the skull in an epidural position (4.0 mm posterior and 3.0 mm left and right to the bregma) by 2 stainless steel screws (M1*2; Hummer and Riess GmbH, Nürnberg, Germany). EEG activity was recorded using a telemetry system (Dataquest A.R.T. Data Acquisition 4.0 for telemetry systems; Data Sciences International), and behavior was monitored using Axis 221 network infrared-sensitive videocameras (Axis Communications AB, Lund, Sweden) with infrared illumination during the dark phase.

The first spontaneous EEG seizure in rats with rating 3 to 4 during SE was observed between 3 and 36 days (mean, 15.3 days) after KA injection; 50% of all rats showed at least 1 spontaneous seizure after 12 days (unpublished data).

Tissue Preparation

For immunohistochemistry, rats were deeply anesthetized by i.p. injection of thiopental (150 mg/kg; Sandoz GmbH, Kundl, Austria) 24 hours (n = 9), 8 days (n = 9), 1 month (n = 10), and 3 months (n = 15) after KA-induced SE. They were then perfused transcardially with phosphate-buffered saline (room temperature [RT], pH 7.4) followed by 80 ml of ice-cold 4% paraformaldehyde in 50-mmol/L phosphate buffer, pH 7.4. Brains were carefully removed from the skulls and postfixed in ice-cold paraformaldehyde for an additional 90 minutes. The brains were then immersed in ice-cold 20% sucrose in 50-mmol/L phosphate buffer for 24 hours, snap-frozen in −70°C isopentane (Merck, Darmstadt, Germany) for 3 minutes and stored at −70°C. Horizontal 30-μm-sections of the ventral hippocampal region were cut on a cryostat microtome (Carl Zeiss AG, Vienna, Austria), collected in 50-μmol/L Tris-buffered saline containing 0.1% NaN_3 (all from Merck), and stored at 4°C.

For ISH, KA-treated rats and age-matched controls were put into a box and killed by exposure to CO_2 at 24 hours (n = 5), 8 days (n = 6), 1 month (n = 5), or 3 months (n = 15) after KA-induced SE. Brains were rapidly removed from the sculls and snap frozen in −70°C isopentane (Merck). Horizontal 20-μm sections were cut using a cryostat microtome, thaw mounted on silane-coated slides, and stored at −70°C.

Nissl Stain

For adjusting the levels of brain sections, every 10th section was collected for Nissl staining. Sections were mounted on slides, dried, dehydrated in graded ethanol series (70%–100%), and transferred to butyl acetate. After rehydration in graded ethanol/H_2O, sections were incubated in 0.5% Cresyl violet (Sigma-Aldrich, St Louis, MO) for 5 minutes and again dehydrated in graded ethanol (70%–100%), transferred to butyl acetate, and coverslipped with Eukitt (O. Kindler GmbH, Freiburg, Germany).

Antibodies

A mouse monoclonal antibody was used for detection of glutamate decarboxylase (GAD67, AB 5406; Chemicon, Temecula, CA); this antibody detects a single band in Western blots of brain extracts (42). An antibody to the vesicular GABA transporter (VGAT, donated by Prof. R. Edwards, University of California at San Francisco, CA) was raised in rabbits against a fusion protein of the N-terminal sequence (99 AA) of VGAT with glutathione S-transferase (43). For CR, a polyclonal antibody (calretinin 7698; SWANT, Marly, Switzerland) was used. The SOM antiserum was raised in rabbits against synthetic SOM-14 coupled to ovalbumin. It recognizes SOM-14 and SOM-28 about equally and was previously characterized (44). The NPY antiserum was raised in rabbit against synthetic porcine NPY (Cambridge Res. Biochemicals, Billingham, UK) coupled to ovalbumin and was previously characterized (45).

Indirect Immunohistochemistry

Free-floating sections were rinsed in 50-mmol/L Tris-buffered saline with 0.1% to 0.4% Triton X-100 (Sigma-Aldrich) for 30 minutes followed by 10% blocking serum (normal goat serum) diluted in TBS-Triton buffer for 90 minutes for reducing nonspecific binding. Sections were then incubated overnight at RT with the primary antibody diluted (VGAT, 1:7500; CR, 1:5000; SOM, 1:2000; NPY, 1:2500) in 10% of blocking serum containing 0.1% NaN_3 and then rinsed 3 times with TBS-Triton for 5 minutes.

Secondary antibodies (P0260 rabbit anti-mouse, 1:200; or P0448 goat anti-rabbit, 1:250; DAKO, Glostrup, Denmark) were diluted with 10% blocking serum in TBS-Triton. Sections were incubated with secondary antibody solution for 150 minutes at RT. After washing 3 times for 5 minutes in TBS buffer, the sections were reacted with 0.05% 3,3′-diaminobenzidine tetrahydrochloride (Sigma-Aldrich) in TBS buffer containing 0.016% H_2O_2. The labeling reaction was monitored under the microscope and stopped by washing the sections in TBS buffer. Sections were mounted on gelatin-coated glass slides in 55% ethanol and allowed to dry overnight. After dehydration in ethanol and clearing in butyl acetate, they were coverslipped with Eukitt embedding medium for light microscopic examination. Omission of the primary antisera served as control and eliminated specific immunoreactivity.

In Situ Hybridization

The following custom-synthesized oligo-DNA probes (Microsynth AG, Balgach, Switzerland) complementary to the respective messenger RNAs (mRNAs) were used: SOM (bases 358–405), 5′-GGA TGT GAA TGT CTT CCA GAA GAA GTT CTT GCA GCC AGC TTT GCG TTC-3′ (NM_012659) (46); NPY (bases 214–259), 5′-CTC TGT CTG GTG ATG AGA TTG ATG TAG TGT CGC AGA GCG GAG TAG T-3 prime; (M15880.1) (47). In situ hybridization was performed as described in detail previously (1). Oligonucleotides (2.5 pmol) were labeled at the 3′-end with [^{35}S] α-thio-dATP (1,300 Ci/mmol; New England Nuclear, Boston, MA) by reaction with terminal deoxynucleotidyltransferase (Roche Austria GmbH, Vienna, Austria) and precipitated with

75% ethanol and 0.4% NaCl. Twenty-micrometer-thick frozen sections were immersed into ice-cold paraformaldehyde (2%) in PBS, pH 7.2 for 10 minutes, rinsed in PBS, immersed in acetic anhydride (0.25% in 0.1-mol/L triethylamine hydrochloride) at RT for 10 minutes, dehydrated by ethanol series, and delipidated with chloroform. The sections were then hybridized in 50-μl hybridization buffer containing about 50 fmol ($0.8–1 \times 10^6$ cpm)-labeled oligonucleotide probe for 18 hours at 42°C. The hybridization buffer consisted of 50% formamide (Merck), 2 × SSC (1 × SSC consisting of 150-mmol/L NaCl and 15-mmol/L sodium citrate, pH 7.2). The sections were then washed twice in 50% formamide in 1 × SSC (42°C, 4 × 15 minutes), briefly rinsed in 1 × SSC, rinsed in water, dipped in 70% ethanol, dried, and then exposed to BioMax MR films (Amersham Pharmacia Biotech, Buckinghamshire, UK) for 8 days (SOM) or 19 days (NPY). After exposure to BioMax MR films, the sections were dipped at 42°C in photosensitive emulsion (NTB-2; Kodak, Rochester, NY) diluted 1:1 with distilled water, air dried, and exposed for 12 days (SOM) or 27 days (NPY). Dipped sections and BioMax MR films were developed using Kodak D19 developer (Kodak). After counterstaining with Cresyl violet, photoemulsion-dipped sections were dehydrated, cleared in butyl acetate, and coverslipped with Eukitt.

Densitometry

For semiquantitative analysis of the density of immune-labeled fibers in the outer molecular layer (oml) of the subiculum, digital 8-bit images from 30-γm-thick immune-labeled slices were taken at a 100-fold magnification with constant illumination and filter settings (OpenLab 4; Perkin-Elmer, Waltham, MA). Images were imported into the image analysis software ImageJ. A rectangle (length, 300 μm; width, 150 μm) with an area of 45,000 μm^2 was placed over the oml of the subiculum, and the average grayscale value of all pixels within the rectangle (8-bit pictures, 256 different gray values: 0 [white]–255 [black]) was measured. The following brain areas were used for determining background labeling: internal capsule for VGAT, ventral part of the medial geniculate nucleus for NPY, and the corpus callosum for SOM and CR. Relative optical densities (RODs) were calculated from gray values according to the following formula: ROD = log (256/[255 − gray value]). The RODs of the left and right hemispheres were averaged, and the ROD of the background was subtracted.

To quantify changes in the intensity of NPY fiber labeling in all parahippocampal subregions, photomicrographs (8 bits) of 30-μm NPY-immunolabeled sections were taken at 100-fold magnification and imported into the ImageJ software. Circles (350 μm diameter) were placed over the regions of interest, and mean gray values of all pixels inside the circles were measured. The following regions were investigated: proximal and distal parts of the subiculum, presubiculum, parasubiculum, superficial and deep layers of the medial and lateral EC, respectively, and perirhinal cortex. Nonspecific background staining was measured in the medial geniculate nucleus. Relative optical densities were calculated as above, and background ROD was subtracted. Relative optical densities of left and right hemispheres were averaged.

Quantification of SOM Neurons in Parahippocampal Areas

To assess the numbers of SOM-immunoreactive (-ir) neurons, photo images of parahippocampal areas (subiculum, presubiculum, parasubiculum, and EC) were obtained from 30-μm sections at 100-fold magnification. Images were imported into the ImageJ software, and areas of interest were manually outlined and measured. Cell numbers within these areas were counted manually, and neuronal densities (neurons/mm^2) were calculated. Numbers obtained in the left and right hemispheres were averaged.

Quantification of NPY mRNA-Expressing Neurons

To quantify the percentage of NPY mRNA-expressing neurons in the subiculum and EC, 20-μm sections were processed for radioactive ISH, dipped in photo emulsion, and counterstained with Cresyl violet. Bright-field microphotographs were taken at 200-fold magnification and imported into the ImageJ software. Circles (350 μm diameter) were placed over the principal cell layers of the proximal and distal parts of the subiculum and over the superficial and deep layers of the medial and lateral EC, respectively. Total numbers of stained neurons inside the circles and neurons expressing NPY mRNA (marked by the accumulation of silver grains) were counted. Percentages of NPY mRNA-expressing neurons were calculated for individual regions.

Quantification of Silver Grains Over NPY and SOM mRNA-Positive Neurons

For quantifying mRNA expression in individual SOM and NPY mRNA-expressing neurons, we determined the number of silver grains located over these cells in sections dipped with photoemulsion after ISH. Dark-field images of the subiculum and the EC were obtained at 200-fold magnification. A threshold for the selective detection of silver grains was set. The areas covered either by SOM or by NPY mRNA-expressing cells (labeled by Nissl stain) including their close vicinity were outlined by 25-μm-diameter circles using the ImageJ software, and the density of silver grains within circles was measured. For SOM mRNA, 1,116 and 1,744 neurons were investigated in the subiculum and the EC, respectively, and 716 and 1,463 were investigated for NPY mRNA in the subiculum and EC, respectively. Densities of individual neurons were averaged for each animal. Statistical analysis was done between groups of animals.

Statistical Analysis

Statistical analysis was carried out using GraphPad Prism 5.0a for Macintosh (GraphPad Software, San Diego, CA). Analysis of variance with Dunnett multiple comparison post hoc test was used for determining between-group differences among multiple sets of data. Correlations were determined by using the Pearson correlation coefficient. All data are presented as mean ± SEM. Statistical significance was defined as $p < 0.05$.

RESULTS

Transient Ectopic Expression of SOM mRNA and Immunoreactivity in Principal Neurons of Parahippocampal Regions

SOM mRNA was restricted to interneurons widely distributed in hippocampal and parahippocampal regions in controls (Fig. 1A). At 24 hours after KA-induced SE, we observed de novo expression of SOM mRNA in pyramidal cells of the hippocampus and parahippocampal areas (Fig. 1B), which extends the observation by Hashimoto and Obata (48) that SOM mRNA is ectopically expressed in pyramidal neurons of hippocampal sectors CA3 and CA1 early (24 hours) after KA-induced SE. De novo expression of SOM mRNA in pyramidal neurons was observed in the subiculum (4/5 rats), parasubiculum (3/5 rats), and in the deep (3/5 rats) and superficial layers of the EC (1/5 rats) at this interval (Figs. 1B, E, I). Expression of SOM mRNA in principal neurons of all parahippocampal subregions was transient, and it was never detected at later intervals (8 days and 1 and 3 months) after KA-induced SE (Figs. 1C, F, J).

Consistent with the de novo expression of SOM mRNA in pyramidal neurons, the numbers of SOM-ir neurons were increased in the subiculum (187% ± 9.1% of controls, $p < 0.001$) and parasubiculum (136% ± 15.9% of controls, $p < 0.01$) but not in the presubiculum and the EC 24 hours after KA injection. Expression of SOM mRNA and SOM-ir in pyramidal

cells were transient, and numbers of SOM-ir cells in the subiculum and parasubiculum returned to control values 8 days after SE (Table 1).

Strikingly, SOM-ir expressed de novo always appeared restricted to the perikarya of principal neurons and diffuse or single-fiber labeling was never observed in the respective target areas of these neurons (stratum oriens and radiatum of the hippocampus proper, pyramidal cell layer and inner molecular layer of the subiculum, or in the deep EC).

Starting at around 8 days after KA, the numbers of SOM-ir interneurons became decreased in the presubiculum (66% ± 5.0% of controls, $p < 0.01$) and in Layers V/VI of the EC (66% ± 5.1% of controls, $p < 0.001$), indicating a loss of these interneurons. At 3 months after KA injection, surviving SOM-ir interneurons seemed to be increased in size in the subiculum but decreased in number (77% ± 2.7% of controls, $p < 0.001$). On the other hand, no significant changes in numbers of SOM-ir neurons were detected in Layer I/II or in Layers III/IV of the EC after 8 days (Table 1).

Increased Expression of SOM mRNA in Surviving Interneurons

In addition to the rapid but transient expression of SOM mRNA in pyramidal neurons of parahippocampal areas, SOM mRNA expression constantly increased in surviving interneurons (Figs. 1C, F). To obtain a measurement of the change in SOM mRNA expression (and thus also for the activity of these neurons), we estimated the density of silver grains (reflecting the amount of mRNA) over individual neurons of the subiculum and EC. In the subiculum (Figs. 1E, F, H), expression of SOM mRNA was already slightly increased in interneurons 24 hours after KA-induced SE (132.3% ± 19.36% of controls; not significant) and later gradually increased to 333.4% ± 24.52% ($p < 0.001$) of controls at 3 months after KA-induced SE (Fig. 1H). In the EC, the changes in SOM mRNA expression were most pronounced in the superficial layers (Layers II–III) (Figs. 2A–D) where the density of silver grains gradually increased to 321.2% ± 16.87% ($p < 0.001$) of controls after 3 months (Fig. 2I). In interneurons of the deep layers of the EC, significantly increased expression of mRNA was detected at 1 month (172.5% ± 22.27% of controls, $p < 0.001$) and 3 months (177.8% ± 19.39% of controls, $p < 0.001$) after KA injection (Fig. 2I). Also in the presubiculum and parasubiculum, surviving SOM neurons expressed increased levels of SOM mRNA and protein at 3 months after KA-induced SE (Figs. 2E–H).

Increased SOM-, NPY-, and VGAT-ir in the Molecular Layer of the Subiculum

In control rats, in addition to the widespread distribution of SOM-ir neurons throughout the hippocampus, the subiculum, presubiculum and parasubiculum, and Layers II to VI of the EC, dense diffuse SOM-ir was present in the stratum lacunosum-moleculare of the hippocampus proper, in the oml of the subiculum (Fig. 3A) and in Layer I of the presubiculum, parasubiculum, and EC, as described by Kohler and Chan-Palay (49).

Labeling of SOM-ir fibers and diffuse SOM-ir (as seen in controls and attributed to SOM interneurons) was reduced in all hippocampal subfields 24 hours after KA-induced seizures. We presume that this is due to the release of the peptide on acute seizures (50); labeling recovered at later intervals. In the oml of the subiculum (the target area of local SOM-containing GABAergic interneurons), diffuse SOM-ir transiently decreased 24 hours after KA-induced seizures (32.8% ± 6.20% of controls, $p < 0.001$) followed by increased SOM-ir at 8 days (104.1% ± 12.62% of controls, $p > 0.05$), 1 month (140.2% ± 13.65% of controls, $p < 0.05$), and 3 months (Figs. 3D, G; 166.3% ± 14.87% of controls, $p < 0.001$). Neuropeptide Y immunoreactivity was significantly increased in the oml of the subiculum at 1 month (201.7% ± 28.82% of controls, $p < 0.01$) and 3 months (218.2% ± 44.00% of controls, $p < 0.001$) after KA-induced SE (Figs. 3B, E, H). Significantly increased levels of

VGAT-ir were observed there at 1 month (152.9% ± 12.77% of control, $p < 0.001$) and at 3 months (210.6% ± 7.39% of controls, $p < 0.001$) after KA-induced SE (Figs. 3C, F, I).

Correlation Between Numbers of Spontaneous Seizures and Labeling Intensity of SOM and CR

In rats subjected to telemetric EEG recording and killed after 3 months, the increase in SOM-ir in the oml of the subiculum positively correlated with the number of spontaneous seizures experienced by these rats (Fig. 4A; $r^2 = 0.3783$, $p = 0.044$, $n = 11$). We recently reported a decrease in CR-ir in the oml of the subiculum due to degeneration of presumably glutamatergic CR-containing fibers arising from the nucleus reuniens thalami (39). The decrease in CR-ir in the oml correlated with the numbers of spontaneous seizures over 3 months (Fig. 4B; $r^2 = 0.4545$, $p = 0.0229$, $n = 11$). To investigate a possible relationship between changes in CR-ir and SOM-ir fibers in the oml of the subiculum, we subjected these parameters to a correlation analysis and observed a strong correlation between the decrease in CR-ir and the increase in SOM-ir ($r^2 = 0.7854$, $p < 0.0001$, $n = 14$; Fig. 4C).

Ectopic NPY mRNA Expression: Increased Numbers of NPY mRNA-Expressing Pyramidal Cells and Increased Expression per Neuron

In controls, NPY mRNA-expressing GABAergic interneurons were detected in all subregions of the hippocampal formation (Fig. 5A) (51). After KA-induced seizures, NPY mRNA expression was altered in a bimodal way. At 24 hours after KA injection, NPY mRNA was not only present in numerous GABAergic interneurons but also highly expressed in dentate granule cells (1), in principal neurons of Layer II and V–VI of the (lateral) EC (4/5 rats), and in pyramidal neurons mainly of the proximal subiculum and hippocampal sector CA1 (3/5 rats) (Fig. 5B). At 8 days after KA injection, the number of NPY mRNA-expressing neurons returned to control levels. Ectopic expression of NPY mRNA was then observed only in 2 of 6 rats and was restricted to dentate granule cells and to neurons in layer V of the EC (not shown). At 1 month and 3 months after KA injection, there was robust expression of NPY mRNA in pyramidal neurons of the subiculum in all investigated rats (Fig. 5C), in principal neurons of Layers II and V of the EC (Figs. 6A, B; 4/8 rats), and in principal neurons of the parasubiculum (Figs. 6E, F; 3/8 rats). In the subiculum, NPY mRNA expression was restricted to pyramidal neurons of the superficial part of its proximal extension at these intervals (Figs. 5G–I).

For quantitative assessment of NPY mRNA expression after KA-induced SE, we determined numbers of NPY mRNA-expressing neurons (per total number of neurons in the respective brain area; Table 2) and the density of silver grains per neuron in photoemulsion-dipped sections after ISH for NPY mRNA (Fig. 7). Although the faint labeling of the neurons did not allow a clear differentiation between principal neurons and interneurons (Fig. 5I), the location of NPY mRNA-containing neurons clearly indicated labeling of interneurons as well as pyramidal cells (Figs. 5H, I). Therefore, we did not differentiate between interneurons and principal neurons expressing NPY mRNA.

The number of NPY mRNA-positive neurons increased in a bimodal way with pronounced peaks after 24 hours and at 1 and 3 months after KA-induced SE. The percentage of NPY mRNA-positive neurons (per total number of neurons) was increased by 6- and 7-fold after 24 hours in the proximal subiculum and superficial EC, respectively. At 8 days, these increases were reduced to 3.8- and 3-fold, and after 1 month, they again reached 12 and 9.7 times increases in the same areas, respectively (Table 2). In the distal subiculum and deep EC, there were also significant increases (between 2.3- and 5.5-fold) in NPY mRNA-expressing neurons (Table 2).

The average density of silver grains detected per neuron was significantly increased in all parahippocampal areas (Fig. 7). Thus, NPY mRNA expression increased by 535%, 204%, and 147% ($p < 0.001$) at 1 to 3 months after KA injection in the subiculum and principal cell layers of the superficial and deep EC, respectively (Fig. 7).

Widespread Epilepsy-Induced Increases in NPY-ir

In controls, NPY-ir neurons were present in all areas of the hippocampal formation of controls as shown by Kohler et al (52) (Fig. 5D). The highest densities of NPY-ir fibers were detected in the oml of the dentate gyrus, in the stratum lacunosum-moleculare of the hippocampus proper, in the oml of the subiculum, and in the superficial layers of the EC (Fig. 5D). As described previously (1), NPY-ir was ectopically expressed in mossy fibers of dentate gyrus 24 hours after KA injection (Fig. 5E) and in pyramidal cells of the distal part of sector CA1 (5/9 rats) (1, 53). Neuropeptide Y–immunoreactive principal neurons were also detected in Layers II and V–VI of the lateral EC in 4 of 9 rats (Fig. 5E).

At 8 days after KA injection, NPY-ir was generally faint throughout the hippocampal formation except for 3 of 9 rats that showed intensive NPY-ir in dentate granule cells, pyramidal neurons of sector CA1 and the subiculum, and in principal neurons of Layers II and Va of the EC (not shown); these rats may have already experienced spontaneous seizures. At this time point, NPY-ir was significantly (~50%) increased in the proximal and distal subiculum, the parasubiculum and Layers II to VI of the lateral EC (Table 3). Neuropeptide Y immunoreactivity progressively increased at 1 and 3 months after KA injection. After 3 months, it was increased by 145% to 180% in different subfields of the subiculum, by 77% to 216% in different layers of the EC, and by 40% to 121% in the presubiculum and parasubiculum, respectively (Table 3). Notably, the increases in NPY-ir were not restricted to hippocampal areas but were seen throughout the brain (not shown). Thus, marked increases in NPY-ir were also seen, for example, in the perirhinal and frontal cortices (Table 3 [45]).

At 1 month after KA injection and thereafter, NPY was also present in axons of these neurons and thus prominently labeled all major excitatory pathways of the hippocampal formation (Fig. 5F). This included not only the terminal areas of mossy fibers in the dentate gyrus and stratum lucidum CA3 but also the terminal areas of Schaffer collaterals in stratum oriens and radiatum of sector CA1, terminals of CA1 pyramidal neuron axons in the pyramidal cell layer and in the inner molecular layer of the subiculum, and fibers arising from pyramidal cells of CA1 and the subiculum and projecting to the deep layers of the EC (Figs. 5F and 6C, D). Moreover, there was a dense plexus of intensely labeled fibers in the parasubiculum (Figs. 6G, H). Strong NPY labeling was also detected in the inner molecular layer of the dentate gyrus, presumably contained in terminals of sprouted mossy fibers. In the subiculum, NPY-ir perikarya of pyramidal neurons were only detected in the superficial part of the pyramidal cell layer of the proximal subiculum (Figs. 5J, K); fiber labeling was most intense in the pyramidal cell layer and in the inner molecular layer of the subiculum (Fig. 5F).

DISCUSSION

We and others previously demonstrated pronounced changes in the expression of SOM and NPY in the dentate gyrus after KA-induced seizures, electrically induced SE and kindling (1, 20, 54–56). Among the most striking observations was the pronounced expression of NPY in granule cells and mossy fibers of epileptic rats (1, 20, 22, 54, 57–59). In the present study, we thoroughly investigated neurochemical and plastic changes involving the neuropeptides SOM and NPY in parahippocampal areas after KA-induced seizures.

The main findings of our present experiments, represented in Figure 8A, are as follows: 1) After KA-induced seizures, SOM is transiently and expressed de novo in pyramidal neurons of the subiculum (besides expression in sectors CA3 and CA1). This is followed by pronounced overexpression in virtually all SOM-containing interneurons of the hippocampal formation and cortical areas. 2) SOM expressed ectopically in principal neurons seems not to be transported into axons. 3) Axon terminals of SOM interneurons, however, express elevated levels of the peptide and presumably sprout in the oml of the subiculum. 4) Numbers of spontaneous seizures experienced over 3 months are positively correlated with the density of SOM-ir fibers and with the decrease in CR-ir in the subiculum. Thus, labeling intensities of SOM and CR are inversely correlated in the molecular layer of the subiculum. 5) After an initial phase of rapid expression of NPY mRNA in granule cells and pyramidal neurons of sector CA1, the peptide is expressed de novo in numerous principal neurons of the hippocampal formation, including pyramidal neurons of the subiculum, the parasubiculum, and the EC with progression of spontaneous seizures. This goes along with pronounced expression of NPY in the respective excitatory pathways of the hippocampal formation and increased tissue levels in parahippocampal regions.

Somatostatin

After KA-induced seizures, the expression of SOM was altered in 2 ways. There was initial transient and ectopic expression of SOM mRNA and immunoreactivity in pyramidal neurons of sectors CA1 and CA3 and of the subiculum and EC. Subsequently, delayed but sustained expression of SOM mRNA and immunoreactivity occurred in interneurons of the entire hippocampal formation and the cerebral cortex.

The rapid expression of SOM in principal neurons may be a direct consequence of the acute SE. Interestingly, it seemed to be restricted to the soma and proximal dendrites and was not detected in axons or in the terminal areas of these neurons (e.g. in the pyramidal cell layer and inner molecular layer of the subiculum or stratum oriens and radiatum of sectors CA3 and CA1). Thus, SOM seemed not to be transported into axons. The reason for this is not clear. Inasmuch as overexpression of the peptide was only transient, it may be merely a problem of detecting it in axons. On the other hand, our antibody, in addition to SOM-14 and SOM-28, also detects prosomatostatin and the hydrated form of SOM with open disulfide bond (60, 61). Thus, it may be possible that due to oxidative stress during epileptic seizures, the formation of the disulfide bond of pre/prosomatostatin is impaired, and thus processing of the propeptide and its transfer into synaptic vesicles would be inhibited. We speculate that this mechanism could contribute to the high vulnerability of pyramidal cells in epilepsy.

Expression of SOM mRNA and immunoreactivity in interneurons increased over time and became most prominent at the later time points after KA injection. Markedly increased mRNA expression was found in interneurons of the entire hippocampal formation, including the subiculum, presubiculum and parasubiculum, and the EC, as well as in the cerebral cortex and other brain areas. The time course for accumulating SOM mRNA expression in interneurons parallels the development of spontaneous seizures. The increases may be caused by recurrent seizure activity and indicate sustained activation of SOM-containing interneurons (1, 50). This is supported by the fact that SOM-ir in terminal areas of subicular interneurons (oml of the subiculum) correlated with the numbers of spontaneous seizures experienced by the rats.

Presumed Sprouting of GABA/SOM Positive Axons in the oml of the Subiculum

Two major types of SOM-containing interneurons have been described in the CA1 sector: stratum oriens/lacunosum-moleculare (O-LM) cells and bistratified cells. The cell bodies of

the O-LM cells are located in stratum oriens and their dendrites extend within the stratum oriens and the alveus for several hundred micrometers (62). The axons of O-LM cells cross the stratum pyramidale and pass through stratum radiatum to stratum lacunosum-moleculare where they form a highly branching plexus (62). They form symmetrical (inhibitory) synapses mainly on distal dendrites of pyramidal neurons in conjunction with asymmetric (excitatory) synapses of presumed entorhinal origin in stratum lacunosum-moleculare (63, 64). Blasco-Ibanez and Freund (65) reported that O-LM cells receive their major excitatory input from local collaterals of CA1 pyramidal cells and concluded that these SOM-containing interneurons are driven primarily in a feedback manner. The other cell type, SOM-containing bistratified cells, have their cell bodies in the stratum pyramidale or adjacent stratum oriens of sector CA1 and innervate pyramidal cell dendrites in the stratum oriens and radiatum (64, 66). They often contain the calcium-binding protein calbindin (67–69). In addition, SOM is also contained in GABA/calbindin neurons projecting to the medial septum and hippocampal interneurons (70, 71).

After the initial increase in the numbers of SOM mRNA-containing neurons (due to its expression in pyramidal cells), we observed reduced numbers of presumable SOM interneurons by ~25% in the subiculum, presumably reflecting a loss in neurons homologous to O-LM cells in CA1. This is in agreement with the previously observed loss of O-LM cells and relative resistance of bistratified SOM/calbindin cells in the pilocarpine model of TLE.

Despite the partial degeneration of SOM neurons, the density of SOM-ir (and that of NPY- and VGAT-ir) in the oml was markedly increased in epileptic rats 3 months after KA-induced SE. Because only cells of the subiculum homologous to O-LM-cells of hippocampal sector CA1 project to the oml of the subiculum and to stratum lacunosum-moleculare of sector CA1 (62, 69), it is most likely that the increased SOM-ir in the oml is contained in axon terminals of these cells (Fig. 8B). This may be due to increased expression of SOM (as indicated by the increased levels of SOM mRNA) in these interneurons.

Massive sprouting of NPY/GABA-containing interneurons has been observed in the subiculum of patients with TLE (17). Thus, the increased labeling of the oml of the subiculum we observed may also reflect axonal sprouting of SOM-containing O-LM cells. However, because of the diffuse labeling with SOM-ir, we were not able to demonstrate this unequivocally in the present study. VGAT-ir was, however, also markedly increased in the oml of the subiculum. VGAT mRNA was not or only negligibly upregulated (not shown), which would suggest axonal sprouting of SOM/GABA neurons in addition to increased expression of SOM. In any case, increased SOM-ir in the oml and increased SOM mRNA in interneurons strongly suggests an increase in the releasable pool of SOM. We speculate that the increased SOM-ir in the oml of the subiculum could also be due to the sprouting bistratified cells of sector CA1 or neurons equivalent to bistratified cells in the subiculum that also contain SOM and putatively innervate pyramidal cell dendrites of the subiculum. These neurons often contain calbindin, but calbindin-ir was not enhanced in KA-treated rats (unpublished observation); this argues against sprouting of SOM-calbindin neurons. An alternative possibility may be that SOM neurons of the thalamus may sprout to the oml of the subiculum and substitute for the loss of CR-ir thalamic-subicular neurons.

Among the SOM receptors, sst1, sst2, and sst4 seem to be most abundant in the brain, including in the hippocampal formation (72–75). Notably, sst2A and sst4 receptors mediate anticonvulsive and antiepileptogenic actions presumably by activating K^+ M currents (32, 33, 76); high concentrations of sst2 are present in the subiculum (73). Thus, sprouted GABA/SOM axon terminals in the oml (or an increased pool of releasable SOM) may exert inhibitory actions through sst2 receptors. The action by SOM, however, may be limited by the rapid internalization of sst2 receptors (74, 77, 78).

Is There an Interaction Between Afferent Thalamic CR-Containing Fibers and Terminals of SOM-Containing O-LM Cells?

Our observation that the increase in SOM-ir in the oml correlated with the previously observed decrease in CR-ir in the same area is striking. Whereas SOM-ir is contained in terminals of GABA-ergic neurons located in the pyramidal layer of the subiculum, presumably homologous to O-LM cells of hippocampal sector CA1 (62), CR-ir is expressed in nerve terminals arising from glutamatergic neurons in the thalamic nucleus reuniens impinging on dendrites of GABAergic interneurons and (to a lesser extent) of pyramidal cells in the subiculum and in sector CA1 (79–81). The 2 events (i.e. degeneration of CR-ir thalamic afferents in the oml and increased expression of SOM-ir [Fig. 8A]) may be only indirectly related. The thalamic CR-positive afferents degenerate early after KA-induced seizures (39). Because the extent of degeneration correlates with spontaneous seizure activity, this event may be causative for the development of spontaneous seizures. On the other hand, upregulation of SOM-ir in the oml occurs late after the initial SE. It may, therefore, be in reverse, triggered by spontaneous seizures. Thus, the net effect of degeneration of afferent thalamic fibers may be proconvulsive (not considering that they also to a lesser extent innervate pyramidal cells) and that of overexpression of SOM anticonvulsive. Because we found a clear correlation of the increase in SOM-ir and the loss in CR-ir, axons of SOM/GABA interneurons might sprout into the area where CR/glutamatergic fibers had degenerated.

Changes in the Expression of NPY

Rapid de novo expression of NPY mRNA and protein in granule cells of the dentate gyrus and in CA1 pyramidal neurons has been widely described as a consequence of epileptic seizures (1, 20, 53, 82, 83). As previously shown using radioimmunoassays and Northern blotting, NPY- and SOM-ir and mRNA expression in the whole hippocampus and frontal cortex occur in a bimodal fashion with an early (24 hours) and a late (1 and 3 months) increase (45, 84, 85). Although ectopic expression of NPY mRNA in principal neurons occurs rapidly after KA-induced seizures (like that for SOM), there is also a slow, steady increase in NPY mRNA expression in interneurons throughout the hippocampal formation and in cortical areas; this contrasts with the fast and transient expression of SOM in principal neurons. This lasting and finally dramatic ectopic upregulation of NPY levels may be triggered by the recurrent spontaneous seizures that become manifest between 1 and 4 weeks after KA injection. This is supported by the recently observed marked increases in NPY and SOM mRNA levels throughout the brain after electrical kindling (20). Our present experiments also reveal that overexpression of NPY is much wider than originally reported. It virtually affects all major excitatory pathways of the hippocampal formation including the mossy fibers and Schaffer collaterals, projections from CA1 to the subiculum and EC, projections from the subiculum and parasubiculum to the EC, and projections from the EC to the perirhinal cortex (Fig. 8C). Notably, the CA1-subiculum border region and the deep and superficial layers of the EC are hyperexcitable in animal models of epilepsy (35, 86) and in human TLE (34, 87). As indicated by the NPY mRNA data, NPY is also widely overexpressed in interneurons.

Together with overexpression of NPY in granule cells/mossy fibers, the expression of its Y2 receptors is also upregulated. The affinity of Y2 receptors presynaptically located on Schaffer collaterals is increased, indicating facilitated transmission of NPY through its Y2 receptors (24, 25, 88). By mediating a closing of N-type Ca^{2+} channels or opening of K^{+} channels, Y2 receptors mediate presynaptic inhibition of glutamate (and NPY) release from terminals of Schaffer collaterals and mossy fibers (27, 89). Indeed, infusions of viral vectors overexpressing NPY or the Y2 receptor have anticonvulsive properties and suppress development of spontaneous seizure activity (29, 31, 90). Considering that neuropeptides are

preferentially released during sustained neuronal stimulation, NPY and SOM may preferentially act during ictal and interictal activity and may suppress developing seizure activity and facilitate termination of seizures through activation of Y2 and sst2 receptors, respectively.

Interestingly, the respective mechanisms are different in human TLE. Thus, in hippocampal specimens of TLE patients, NPY is not expressed in principal neurons, although Y2 receptors are widely upregulated, including in the subiculum (17). In addition, in specimens with Ammon horn sclerosis, massive sprouting is observed throughout the dentate gyrus, hippocampus proper, and, most pronounced, in the subiculum. This indicates that in human TLE, endogenous NPY released from interneurons on Y2 receptors located on terminals of glutamatergic neurons may have an anticonvulsive role by inhibiting release of glutamate (28).

In summary, overexpression of both NPY and SOM indicates lasting activation and plasticity of parahippocampal areas by recurrent seizures. The 2 peptides are preferentially released during high-frequency stimulation, thus in the ictal phase they may contribute to termination of acute seizures. As an important epileptogenic area (34–36) and main output region of the hippocampus, the subiculum may have an important role in these mechanisms. The respective peptide receptors, NPY-Y2 and sst2 receptors, may be valuable targets for future antiepileptic therapy, as shown by proof-of-principle experiments in applying viral vectors overexpressing NPY in epileptic rats (29, 31).

Acknowledgments

The authors thank Elisabeth Gasser for excellent technical assistance.

This research was supported by the Austrian Research Funds (Grant No. P19464) and by the European Union Grant FP6 EPICURE (LSH-CT-2006-037315).

REFERENCES

1. Sperk G, Marksteiner J, Gruber B, et al. Functional changes in neuropeptide Y– and somatostatin-containing neurons induced by limbic seizures in the rat. Neuroscience. 1992; 50:831–46. [PubMed: 1360155]
2. Dragunow M, Yamada N, Bilkey DK, et al. Induction of immediate-early gene proteins in dentate granule cells and somatostatin interneurons after hippocampal seizures. Brain Res Mol Brain Res. 1992; 13:119–26. [PubMed: 1349720]
3. Binder DK, Croll SD, Gall CM, et al. BDNF and epilepsy: Too much of a good thing? Trends Neurosci. 2001; 24:47–53. [PubMed: 11163887]
4. Tsunashima K, Schwarzer C, Kirchmair E, et al. GABA(A) receptor subunits in the rat hippocampus. III: Altered messenger RNA expression in kainic acid–induced epilepsy. Neuroscience. 1997; 80:1019–32. [PubMed: 9284057]
5. Sperk G, Schwarzer C, Tsunashima K, et al. Expression of GABA(A) receptor subunits in the hippocampus of the rat after kainic acid–induced seizures. Epilepsy Res. 1998; 32:129–39. [PubMed: 9761315]
6. Sutula T, Cascino G, Cavazos J, et al. Mossy fiber synaptic reorganization in the epileptic human temporal lobe. Ann Neurol. 1989; 26:321–30. [PubMed: 2508534]
7. Cavazos JE, Golarai G, Sutula TP. Mossy fiber synaptic reorganization induced by kindling: Time course of development, progression, and permanence. J Neurosci. 1991; 11:2795–803. [PubMed: 1880549]
8. Represa A, Le Gall La Salle G, Ben-Ari Y. Hippocampal plasticity in the kindling model of epilepsy in rats. Neurosci Lett. 1989; 99:345–50. [PubMed: 2542847]

9. Siddiqui AH, Joseph SA. CA3 axonal sprouting in kainate-induced chronic epilepsy. Brain Res. 2005; 1066:129–46. [PubMed: 16359649]
10. Smith BN, Dudek FE. Short- and long-term changes in CA1 network excitability after kainate treatment in rats. J Neurophysiol. 2001; 85:1–9. [PubMed: 11152700]
11. Perez Y, Morin F, Beaulieu C, et al. Axonal sprouting of CA1 pyramidal cells in hyperexcitable hippocampal slices of kainate-treated rats. Eur J Neurosci. 1996; 8:736–48. [PubMed: 9081625]
12. Lehmann TN, Gabriel S, Kovacs R, et al. Alterations of neuronal connectivity in area CA1 of hippocampal slices from temporal lobe epilepsy patients and from pilocarpine-treated epileptic rats. Epilepsia. 2000; 41(Suppl 6):S190–94. [PubMed: 10999543]
13. Esclapez M, Hirsch JC, Ben-Ari Y, et al. Newly formed excitatory pathways provide a substrate for hyperexcitability in experimental temporal lobe epilepsy. J Comp Neurol. 1999; 408:449–60. [PubMed: 10340497]
14. Cavazos JE, Jones SM, Cross DJ. Sprouting and synaptic reorganization in the subiculum and CA1 region of the hippocampus in acute and chronic models of partial-onset epilepsy. Neuroscience. 2004; 126:677–88. [PubMed: 15183517]
15. Blumcke I, Beck H, Nitsch R, et al. Preservation of calretinin-immunoreactive neurons in the hippocampus of epilepsy patients with Ammon's horn sclerosis. J Neuropathol Exp Neurol. 1996; 55:329–41. [PubMed: 8786391]
16. de Lanerolle NC, Kim JH, Robbins RJ, et al. Hippocampal interneuron loss and plasticity in human temporal lobe epilepsy. Brain Res. 1989; 495:387–95. [PubMed: 2569920]
17. Furtinger S, Pirker S, Czech T, et al. Plasticity of Y1 and Y2 receptors and neuropeptide Y fibers in patients with temporal lobe epilepsy. J Neurosci. 2001; 21:5804–12. [PubMed: 11466452]
18. Mathern GW, Babb TL, Pretorius JK, et al. Reactive synaptogenesis and neuron densities for neuropeptide Y, somatostatin, and glutamate decarboxylase immunoreactivity in the epileptogenic human fascia dentata. J Neurosci. 1995; 15:3990–4004. [PubMed: 7751960]
19. Gruber B, Greber S, Rupp E, et al. Differential NPY mRNA expression in granule cells and interneurons of the rat dentate gyrus after kainic acid injection. Hippocampus. 1994; 4:474–82. [PubMed: 7874238]
20. Schwarzer C, Sperk G, Samanin R, et al. Neuropeptides-immunoreactivity and their mRNA expression in kindling: Functional implications for limbic epileptogenesis. Brain Res Brain Res Rev. 1996; 22:27–50. [PubMed: 8871784]
21. Takahashi Y, Tsunashima K, Sadamatsu M, et al. Altered hippocampal expression of neuropeptide Y, somatostatin, and glutamate decarboxylase in Ihara's epileptic rats and spontaneously epileptic rats. Neurosci Lett. 2000; 287:105–8. [PubMed: 10854723]
22. Vezzani A, Schwarzer C, Lothman EW, et al. Functional changes in somatostatin and neuropeptide Y containing neurons in the rat hippocampus in chronic models of limbic seizures. Epilepsy Res. 1996; 26:267–79. [PubMed: 8985706]
23. Tsunashima K, Sadamatsu M, Takahashi Y, et al. Trimethyltin intoxication induces marked changes in neuropeptide expression in the rat hippocampus. Synapse. 1998; 29:333–42. [PubMed: 9661251]
24. Schwarzer C, Kofler N, Sperk G. Up-regulation of neuropeptide Y-Y2 receptors in an animal model of temporal lobe epilepsy. Mol Pharmacol. 1998; 53:6–13. [PubMed: 9443927]
25. Gobbi M, Gariboldi M, Piwko C, et al. Distinct changes in peptide YY binding to, and mRNA levels of, Y1 and Y2 receptors in the rat hippocampus associated with kindling epileptogenesis. J Neurochem. 1998; 70:1615–22. [PubMed: 9523578]
26. El Bahh B, Balosso S, Hamilton T, et al. The anti-epileptic actions of neuropeptide Y in the hippocampus are mediated by Y and not Y receptors. Eur J Neurosci. 2005; 22:1417–30. [PubMed: 16190896]
27. Greber S, Schwarzer C, Sperk G. Neuropeptide Y inhibits potassium-stimulated glutamate release through Y2 receptors in rat hippocampal slices in vitro. Br J Pharmacol. 1994; 113:737–40. [PubMed: 7858862]
28. Patrylo PR, van den Pol AN, Spencer DD, et al. NPY inhibits glutamatergic excitation in the epileptic human dentate gyrus. J Neurophysiol. 1999; 82:478–83. [PubMed: 10400974]

29. Richichi C, Lin EJ, Stefanin D, et al. Anticonvulsant and antiepileptogenic effects mediated by adeno-associated virus vector neuropeptide Y expression in the rat hippocampus. J Neurosci. 2004; 24:3051–59. [PubMed: 15044544]
30. Klapstein GJ, Colmers WF. Neuropeptide Y suppresses epileptiform activity in rat hippocampus in vitro. J Neurophysiol. 1997; 78:1651–61. [PubMed: 9310450]
31. Noe F, Pool AH, Nissinen J, et al. Neuropeptide Y gene therapy decreases chronic spontaneous seizures in a rat model of temporal lobe epilepsy. Brain. 2008; 131:1506–15. [PubMed: 18477594]
32. Tallent MK, Siggins GR. Somatostatin acts in CA1 and CA3 to reduce hippocampal epileptiform activity. J Neurophysiol. 1999; 81:1626–35. [PubMed: 10200199]
33. Vezzani A, Hoyer D. Brain somatostatin: A candidate inhibitory role in seizures and epileptogenesis. Eur J Neurosci. 1999; 11:3767–76. [PubMed: 10583466]
34. Cohen I, Navarro V, Clemenceau S, et al. On the origin of interictal activity in human temporal lobe epilepsy in vitro. Science. 2002; 298:1418–21. [PubMed: 12434059]
35. Knopp A, Kivi A, Wozny C, et al. Cellular and network properties of the subiculum in the pilocarpine model of temporal lobe epilepsy. J Comp Neurol. 2005; 483:476–88. [PubMed: 15700275]
36. de Guzman P, Inaba Y, Baldelli E, et al. Network hyperexcitability within the deep layers of the pilocarpine-treated rat entorhinal cortex. J Physiol. 2008; 586:1867–83. [PubMed: 18238812]
37. Du F, Whetsell WO Jr, Abou-Khalil B, et al. Preferential neuronal loss in Layer III of the entorhinal cortex in patients with temporal lobe epilepsy. Epilepsy Res. 1993; 16:223–33. [PubMed: 8119273]
38. Thom M, Zhou J, Martinian L, et al. Quantitative post-mortem study of the hippocampus in chronic epilepsy: Seizures do not inevitably cause neuronal loss. Brain. 2005; 128:1344–57. [PubMed: 15758032]
39. Drexel M, Preidt AP, Kirchmair E, et al. Parvalbumin interneurons and calretinin fibers arising from the thalamic nucleus reuniens degenerate in the subiculum after kainic acid–induced seizures. Neuroscience. 2011; 189:316–29. [PubMed: 21616128]
40. Du F, Eid T, Lothman EW, et al. Preferential neuronal loss in Layer III of the medial entorhinal cortex in rat models of temporal lobe epilepsy. J Neurosci. 1995; 15:6301–13. [PubMed: 7472396]
41. Sperk G, Lassmann H, Baran H, et al. Kainic acid induced seizures: Neurochemical and histopathological changes. Neuroscience. 1983; 10:1301–15. [PubMed: 6141539]
42. Sperk G, Wieselthaler-Holzl A, Pirker S, et al. Glutamate decarboxylase67 is expressed in hippocampal mossy fibers of temporal lobe epilepsy patients. Hippocampus. 2012; 22:590–603. [PubMed: 21509853]
43. Chaudhry FA, Reimer RJ, Bellocchio EE, et al. The vesicular GABA transporter, VGAT, localizes to synaptic vesicles in sets of glycinergic as well as GABAergic neurons. J Neurosci. 1998; 18:9733–50. [PubMed: 9822734]
44. Sperk G, Widmann R. Somatostatin precursor in the rat striatum: Changes after local injection of kainic acid. J Neurochem. 1985; 45:1441–47. [PubMed: 2864394]
45. Marksteiner J, Sperk G. Concomitant increase of somatostatin, neuropeptide Y and glutamate decarboxylase in the frontal cortex of rats with decreased seizure threshold. Neuroscience. 1988; 26:379–85. [PubMed: 2902535]
46. Goodman RH, Jacobs JW, Dee PC, et al. Somatostatin-28 encoded in a cloned cDNA obtained from a rat medullary thyroid carcinoma. J Biol Chem. 1982; 257:1156–59. [PubMed: 6120163]
47. Larhammar D, Ericsson A, Persson H. Structure and expression of the rat neuropeptide Y gene. Proc Natl Acad Sci U S A. 1987; 84:2068–72. [PubMed: 3031663]
48. Hashimoto T, Obata K. Induction of somatostatin by kainic acid in pyramidal and granule cells of the rat hippocampus. Neurosci Res. 1991; 12:514–27. [PubMed: 1686645]
49. Kohler C, Chan-Palay V. Somatostatin and vasoactive intestinal polypeptide-like immunoreactive cells and terminals in the retrohippocampal region of the rat brain. Anat Embryol (Berl). 1983; 167:151–72. [PubMed: 6137169]
50. Sperk G, Wieser R, Widmann R, et al. Kainic acid induced seizures: Changes in somatostatin, substance P and neurotensin. Neuroscience. 1986; 17:1117–26. [PubMed: 2423920]

51. Morris BJ. Neuronal localisation of neuropeptide Y gene expression in rat brain. J Comp Neurol. 1989; 290:358–68. [PubMed: 2592617]
52. Kohler C, Eriksson L, Davies S, et al. Neuropeptide Y innervation of the hippocampal region in the rat and monkey brain. J Comp Neurol. 1986; 244:384–400. [PubMed: 3514690]
53. Gall C, Lauterborn J, Isackson P, et al. Seizures, neuropeptide regulation, and mRNA expression in the hippocampus. Prog Brain Res. 1990; 83:371–90. [PubMed: 2203104]
54. Schwarzer C, Williamson JM, Lothman EW, et al. Somatostatin, neuropeptide Y, neurokinin B and cholecystokinin immunoreactivity in two chronic models of temporal lobe epilepsy. Neuroscience. 1995; 69:831–45. [PubMed: 8596652]
55. Kato N, Higuchi T, Friesen HG, et al. Changes of immunoreactive somatostatin and beta-endorphin content in rat brain after amygdaloid kindling. Life Sci. 1983; 32:2415–22. [PubMed: 6134222]
56. Pitkanen A, Jolkkonen J, Honkanen KL, et al. Effect of pentylenetetrazol-induced convulsions on somatostatin-like immunoreactivity in rat cerebro-spinal fluid. Neuropeptides. 1987; 9:19–24. [PubMed: 2882440]
57. Chafetz RS, Nahm WK, Noebels JL. Aberrant expression of neuropeptide Y in hippocampal mossy fibers in the absence of local cell injury following the onset of spike-wave synchronization. Brain Res Mol Brain Res. 1995; 31:111–21. [PubMed: 7476019]
58. Arabadzisz D, Antal K, Parpan F, et al. Epileptogenesis and chronic seizures in a mouse model of temporal lobe epilepsy are associated with distinct EEG patterns and selective neurochemical alterations in the contralateral hippocampus. Exp Neurol. 2005; 194:76–90. [PubMed: 15899245]
59. Sperk G, Hamilton T, Colmers WF. Neuropeptide Y in the dentate gyrus. Prog Brain Res. 2007; 163:285–97. [PubMed: 17765725]
60. Strieder G, Sperk G. Purification and characterization of prosomatostatin from rat brain. J Neurochem. 1989; 53:346–53. [PubMed: 2568402]
61. Widmann R, Maas D, Sperk G. Effect of local injection of cysteamine and cystamine on somatostatin and neuropeptide Y levels in the rat striatum. J Neurochem. 1988; 50:1682–86. [PubMed: 2897423]
62. McBain CJ, DiChiara TJ, Kauer JA. Activation of metabotropic glutamate receptors differentially affects two classes of hippocampal interneurons and potentiates excitatory synaptic transmission. J Neurosci. 1994; 14:4433–45. [PubMed: 7517996]
63. Freund TF, Buzsaki G. Interneurons of the hippocampus. Hippocampus. 1996; 6:347–470. [PubMed: 8915675]
64. Katona I, Acsady L, Freund TF. Postsynaptic targets of somatostatin-immunoreactive interneurons in the rat hippocampus. Neuroscience. 1999; 88:37–55. [PubMed: 10051188]
65. Blasco-Ibanez JM, Freund TF. Synaptic input of horizontal interneurons in stratum oriens of the hippocampal CA1 subfield: Structural basis of feed-back activation. Eur J Neurosci. 1995; 7:2170–80. [PubMed: 8542073]
66. Maccaferri G, Roberts JD, Szucs P, et al. Cell surface domain specific postsynaptic currents evoked by identified GABAergic neurones in rat hippocampus in vitro. J Physiol. 2000; 524:91–116. [PubMed: 10747186]
67. Dinocourt C, Petanjek Z, Freund TF, et al. Loss of interneurons innervating pyramidal cell dendrites and axon initial segments in the CA1 region of the hippocampus following pilocarpine-induced seizures. J Comp Neurol. 2003; 459:407–25. [PubMed: 12687707]
68. Sik A, Penttonen M, Buzsaki G. Interneurons in the hippocampal dentate gyrus: An in vivo intracellular study. Eur J Neurosci. 1997; 9:573–88. [PubMed: 9104599]
69. Sik A, Penttonen M, Ylinen A, et al. Hippocampal CA1 interneurons: An in vivo intracellular labeling study. J Neurosci. 1995; 15:6651–65. [PubMed: 7472426]
70. Gulyas AI, Hajos N, Katona I, et al. Interneurons are the local targets of hippocampal inhibitory cells which project to the medial septum. Eur J Neurosci. 2003; 17:1861–72. [PubMed: 12752786]
71. Toth K, Freund TF. Calbindin D28k-containing nonpyramidal cells in the rat hippocampus: Their immunoreactivity for GABA and projection to the medial septum. Neuroscience. 1992; 49:793–805. [PubMed: 1279455]

72. Hervieu G, Emson PC. The localization of somatostatin receptor 1 (sst1) immunoreactivity in the rat brain using an N-terminal specific antibody. Neuroscience. 1998; 85:1263–84. [PubMed: 9681962]
73. Schindler M, Sellers LA, Humphrey PP, et al. Immunohistochemical localization of the somatostatin SST2(A) receptor in the rat brain and spinal cord. Neuroscience. 1997; 76:225–40. [PubMed: 8971774]
74. Schreff M, Schulz S, Handel M, et al. Distribution, targeting, and internalization of the sst4 somatostatin receptor in rat brain. J Neurosci. 2000; 20:3785–97. [PubMed: 10804219]
75. Selmer IS, Schindler M, Humphrey PP, et al. First localisation of somatostatin sst(4) receptor protein in selected human brain areas: An immunohistochemical study. Brain Res Mol Brain Res. 2000; 82:114–25. [PubMed: 11042364]
76. Tallent MK, Qiu C. Somatostatin: An endogenous antiepileptic. Mol Cell Endocrinol. 2008; 286:96–103. [PubMed: 18221832]
77. Csaba Z, Richichi C, Bernard V, et al. Plasticity of somatostatin and somatostatin sst2A receptors in the rat dentate gyrus during kindling epileptogenesis. Eur J Neurosci. 2004; 19:2531–38. [PubMed: 15128406]
78. Csaba Z, Pirker S, Lelouvier B, et al. Somatostatin receptor type 2 undergoes plastic changes in the human epileptic dentate gyrus. J Neuropathol Exp Neurol. 2005; 64:956–69. [PubMed: 16254490]
79. Wouterlood FG, Saldana E, Witter MP. Projection from the nucleus reuniens thalami to the hippocampal region: Light and electron microscopic tracing study in the rat with the anterograde tracer *Phaseolus vulgaris*-leucoagglutinin. J Comp Neurol. 1990; 296:179–203. [PubMed: 2358531]
80. Dolleman-Van Der Weel MJ, Witter MP. Projections from the nucleus reuniens thalami to the entorhinal cortex, hippocampal field CA1, and the subiculum in the rat arise from different populations of neurons. J Comp Neurol. 1996; 364:637–50. [PubMed: 8821451]
81. Bokor H, Csaki A, Kocsis K, et al. Cellular architecture of the nucleus reuniens thalami and its putative aspartatergic/glutamatergic projection to the hippocampus and medial septum in the rat. Eur J Neurosci. 2002; 16:1227–39. [PubMed: 12405983]
82. Lurton D, Cavalheiro EA. Neuropeptide-Y immunoreactivity in the pilocarpine model of temporal lobe epilepsy. Exp Brain Res. 1997; 116:186–90. [PubMed: 9305828]
83. Marksteiner J, Ortler M, Bellmann R, et al. Neuropeptide Y biosynthesis is markedly induced in mossy fibers during temporal lobe epilepsy of the rat. Neurosci Lett. 1990; 112:143–48. [PubMed: 2359514]
84. Bellmann R, Widmann R, Olenik C, et al. Enhanced rate of expression and biosynthesis of neuropeptide Y after kainic acid–induced seizures. J Neurochem. 1991; 56:525–30. [PubMed: 1988555]
85. Marksteiner J, Sperk G, Maas D. Differential increases in brain levels of neuropeptide Y and vasoactive intestinal polypeptide after kainic acid-induced seizures in the rat. Naunyn Schmiedebergs Arch Pharmacol. 1989; 339:173–77. [PubMed: 2566924]
86. de Guzman P, Inaba Y, Biagini G, et al. Subiculum network excitability is increased in a rodent model of temporal lobe epilepsy. Hippocampus. 2006; 16:843–60. [PubMed: 16897722]
87. Wozny C, Knopp A, Lehmann TN, et al. The subiculum: A potential site of ictogenesis in human temporal lobe epilepsy. Epilepsia. 2005; 46(suppl 5):17–21. [PubMed: 15987248]
88. Roder C, Schwarzer C, Vezzani A, et al. Autoradiographic analysis of neuropeptide Y receptor binding sites in the rat hippocampus after kainic acid–induced limbic seizures. Neuroscience. 1996; 70:47–55. [PubMed: 8848135]
89. Colmers WF, Lukowiak K, Pittman QJ. Neuropeptide Y action in the rat hippocampal slice: Site and mechanism of presynaptic inhibition. J Neurosci. 1988; 8:3827–37. [PubMed: 2848110]
90. Woldbye DP, Angehagen M, Gotzsche CR, et al. Adeno-associated viral vector–induced overexpression of neuropeptide Y Y2 receptors in the hippocampus suppresses seizures. Brain. 2010; 133:2778–88. [PubMed: 20688813]

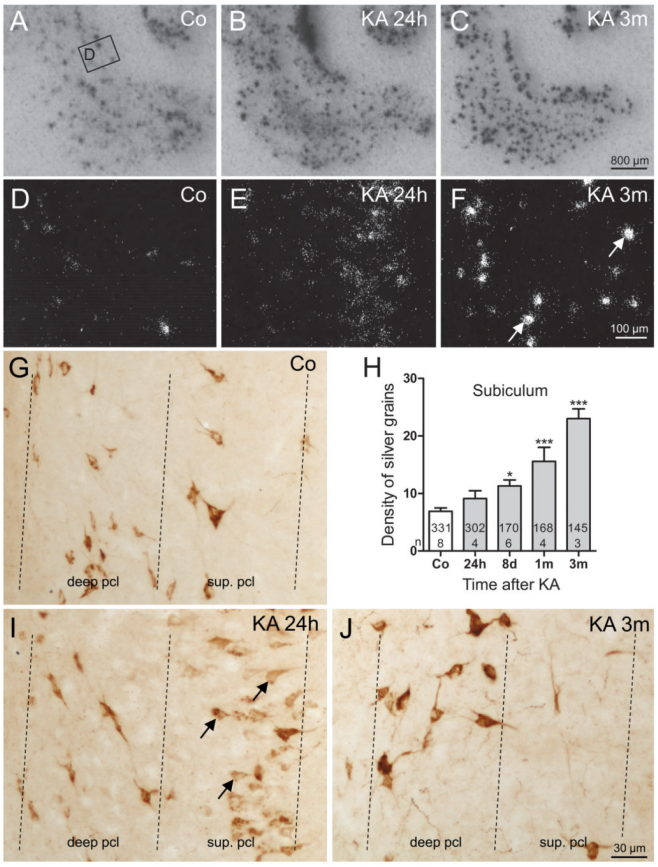

FIGURE 1.

Changes in the expression of somatostatin (SOM) mRNA and immunoreactivity after kainic acid (KA)-induced status epilepticus (SE). **(A–C)** Transient de novo expression of SOM mRNA is induced in principal neurons of the parahippocampal region (subiculum, parasubiculum, entorhinal cortex [EC]) 24 hours after KA-induced SE shown in autoradiograms after in situ hybridization. **(D–F)** High-magnification dark-field images of photoemulsion-dipped sections after in situ hybridization. In the subiculum of a control (Co), SOM mRNA is expressed in γ-aminobutyric acid (GABA)-ergic interneurons located in the pyramidal cell layer **(D)**. Early after KA-induced seizures (24 hours), SOM mRNA is transiently expressed in pyramidal neurons of the proximal subiculum **(E)**. At 3 months (3m), greater levels of SOM mRNA are observed in surviving GABAergic interneurons of the subiculum **(F)**. **(G–J)** Quantification of density of silver grains in photoemulsion-dipped sections after radioactive in situ hybridization revealed increased expression of SOM mRNA in surviving SOM interneurons in the subiculum **(H)**. Statistical analysis was done using analysis of variance with Dunnett multiple comparison post hoc test between treated animals and controls. *, $p < 0.05$; ***, $p < 0.001$. The numbers of neurons and the numbers of animals investigated per group are shown in the columns. **(G, I, J)** High-magnification images of SOM-immunoreactive neurons in the pyramidal cell layer. Note that in the control, SOM is restricted to interneurons **(G)**. At 24 hours after KA, there is strong expression of SOM in pyramidal cells of the subiculum **(I)** that disappears at 3m **(J)**. SOM immunoreactivity is mainly confined to pyramidal cell somata and their proximal dendrites at 24 hours **(I)**.

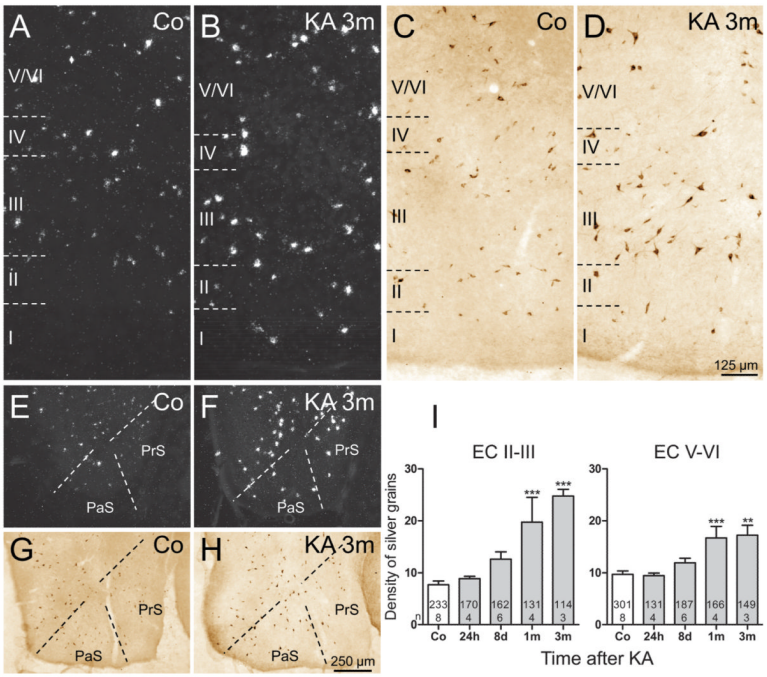

FIGURE 2.

Expression of somatostatin (SOM) mRNA and immunoreactivity in the presubiculum (PrS), parasubiculum (PaS), and entorhinal cortex (EC) of controls and epileptic rats. **(A, B)** Expression of SOM mRNA was increased in all layers of the EC 3 months after kainic acid (KA) injection. **(C, D)** Accordingly, SOM immunoreactivity was increased in surviving neurons in the EC. **(E–H)** SOM mRNA levels **(E, F)** and SOM-immunoreactivity **(G, H)** were also increased in the presubiculum and parasubiculum at 3 months after KA-induced status epilepticus (SE). Quantification of the density of silver grains above neurons of the Layers II–III and V–VI of the EC in photoemulsion-dipped sections after radioactive in situ hybridization **(I)** reveals a progressive increase of SOM mRNA levels within individual neurons after KA-induced SE. Analysis of variance with Dunnett multiple comparison post hoc test between treated animals and controls. **, $p < 0.01$; ***, $p < 0.001$. The numbers of neurons and the numbers of animals investigated per group are shown in the columns.

Europe PMC Funders Author Manuscripts

Europe PMC Funders Author Manuscripts

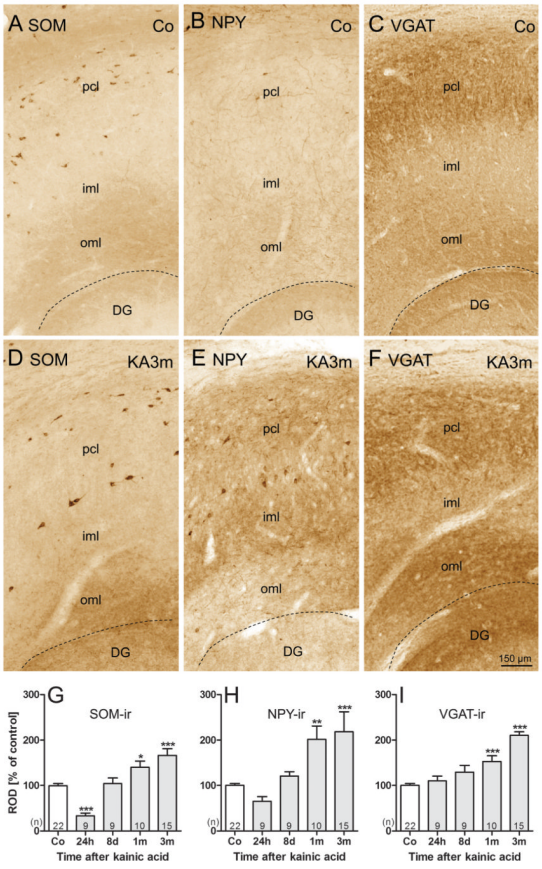

FIGURE 3.

Increased somatostatin (SOM), neuropeptide Y (NPY), and vesicular GABA transporter (VGAT) immunoreactivity (-ir) in the outer molecular layer (oml) of the subiculum of epileptic rats. Representative high-magnification photomicrographs of sections of the subiculum labeled for SOM-, NPY-, and VGAT-ir, respectively, are shown for controls **(A–C)** and epileptic rats at 3 months after kainic acid (KA) injections **(D–F)**. Labeling of SOM-containing fibers and nerve terminals was increased in the oml of the subiculum at 3 months after KA-induced status epilepticus (SE) **(A, D)**. At this time point, NPY-ir was increased in all layers of the subiculum **(B, E)**. Labeling for the vesicular γ-aminobutyric acid (GABA) transporter VGAT was concomitantly increased in the oml of the subiculum **(C, F)**. Note also the markedly enhanced labeling of SOM-ir **(D)** and NPY-ir **(E)** interneurons at 3 months after KA. Densitometry of immunoreactivities in the oml reveal initially decreased (24 hours) but later increased immunostaining for SOM **(G)** and NPY **(H)**. VGAT-ir in the oml of the subiculum **(I)** gradually increased after KA-induced SE. The initial decrease in SOM- and NPY-ir may be due to massive release of the peptides during SE. Statistical analysis was done using analysis of variance and Dunnett multiple comparison post hoc test for comparing KA-injected and control rats. *, $p < 0.05$; **, $p < 0.01$; ***, $p < 0.001$. Animal numbers are given in columns; dashed lines indicate the hippocampal fissure. DG, dentate gyrus; iml, inner molecular layer; oml, outer molecular layer; pcl, pyramidal cell layer.

Europe PMC Funders Author Manuscripts

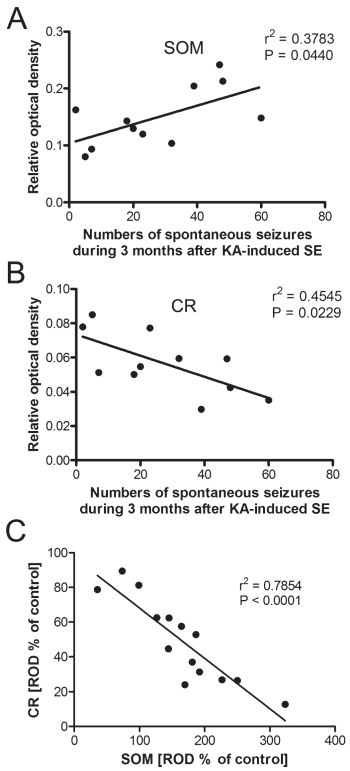

FIGURE 4.

Correlations between numbers of spontaneous epileptic seizures and immunolabeling for somatostatin (SOM) and calretinin (CR) in the subiculum. **(A, B)** The intensity of SOM labeling in the outer molecular layer of the subiculum was positively correlated with numbers of spontaneous seizures experienced for 3 months **(A)**, but the intensity of CR labeling was negatively correlated with seizure numbers **(B)**. **(C)** Labeling intensities of SOM- and CR-immunoreactivity revealed a strong inverse correlation in this layer (Pearson correlation coefficient).

Europe PMC Funders Author Manuscripts

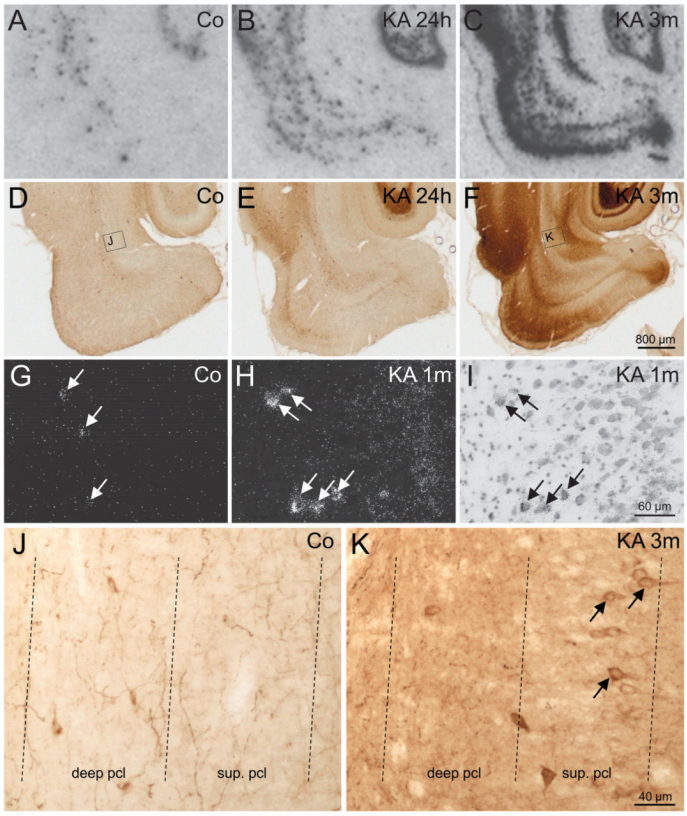

FIGURE 5.

Widespread changes in neuropeptide Y (NPY) mRNA expression and immunoreactivity in epileptic rats. **(A–F)** Images of film autoradiographs of parahippocampal areas of controls (Co) and following kainic acid (KA)–induced seizures after in situ hybridization for NPY mRNA **(A–C)** and NPY immunoreactivity (-ir) in the same areas **(D–F)**. Neuropeptide Y mRNA expression and immunolabeling are increased in the parahippocampal region at 24 hours after KA-induced seizures **(B, E)**. At 3 months after KA injection, de novo expression of NPY mRNA is observed in principal neurons of the subiculum, parasubiculum, entorhinal cortex (EC), and perirhinal cortex **(C)**, and intensely labeled NPY-containing fibers are present throughout the parahippocampal areas **(F)**. **(G–I)** High-magnification photomicrographs of photoemulsion-dipped sections after in situ hybridization for NPY mRNA show the pyramidal cell layer of the proximal subiculum of control **(G)** and 1 month after status epilepticus (SE) (**H**, dark-field; **I**, bright-field). In controls, NPY mRNA is only expressed in interneurons (arrows in **G**). In epileptic rats, interneurons express increased levels of NPY mRNA (arrows in **H** and **I**). Moreover, NPY is also expressed de novo in numerous pyramidal neurons of the subiculum **(H, I)**. **(J, K)** High-magnification photomicrographs of the subicular pyramidal cell layer reveal NPY-ir pyramidal cells at 3 months after KA (**K**, arrows) but not in controls (**J**; note NPY-ir fibers).

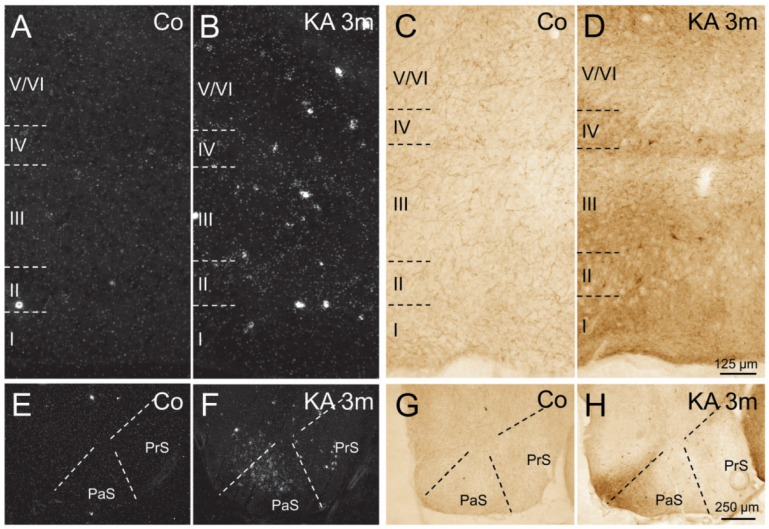

FIGURE 6.

Epilepsy-induced changes in neuropeptide Y (NPY) mRNA expression and immunolabeling in the presubiculum (PrS), parasubiculum (PaS), and entorhinal cortex (EC). **(A, B)** In situ hybridization reveals increased numbers of NPY mRNA-expressing neurons in Layers I to VI of the EC of an epileptic rat 3 months after status epilepticus (SE) versus control (Co). **(C, D)** There are increased densities of NPY-immunoreactive neurons and fibers in all layers of the epileptic EC. **(E, F)** Increased numbers of NPY mRNA-expressing neurons are also present in the PrS and especially in the PaS of epileptic rats. **(G, H)** Labeling of NPY-containing fibers is increased in the PaS but not in the PrS of epileptic rats.

Europe PMC Funders Author Manuscripts

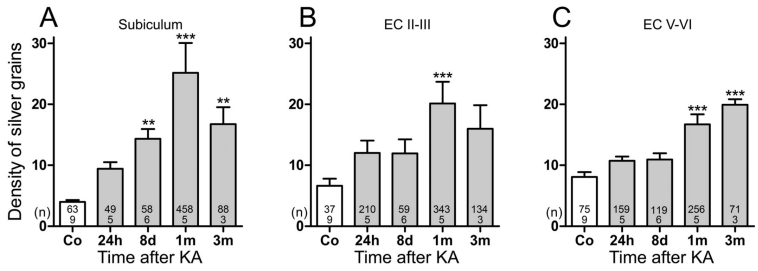

FIGURE 7.

Time course of increases in neuropeptide Y (NPY) mRNA expression in the subiculum and entorhinal cortex (EC). **(A–C)** Numbers of silver grains were estimated above NPY mRNA-expressing neurons in sections processed for in situ hybridization. Data are shown for the subiculum **(A)**, Layers II/III **(B)**, and V/VI **(C)** of the EC. Statistical analysis was done using analysis of variance and Dunnett multiple comparison post hoc test for comparing kainic acid (KA)–injected and control rats. **, $p < 0.01$; ***, $p < 0.001$. Numbers of rats per group and numbers of neurons evaluated per group are shown within the bars.

Europe PMC Funders Author Manuscripts

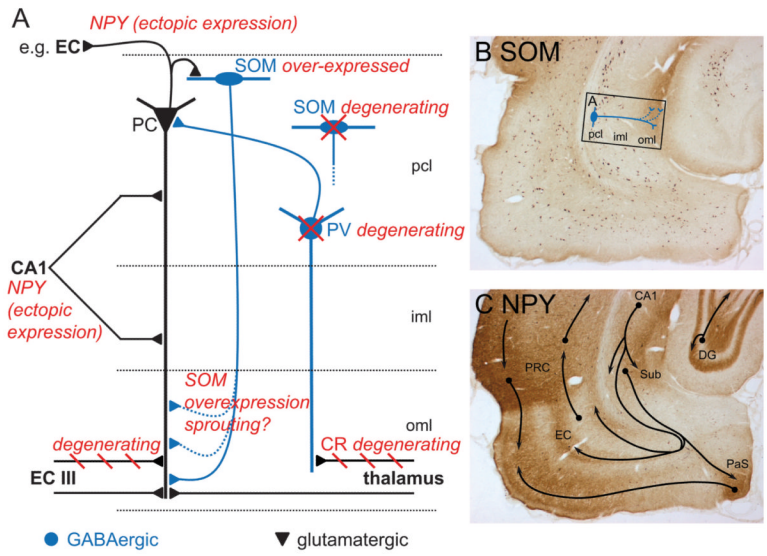

FIGURE 8.

Long-term changes in parahippocampal regions after kainic acid (KA)–induced status epilepticus (SE). **(A)** Scheme illustrating the main changes in neuropeptide systems in the subiculum 3 months after KA-induced SE. Glutamatergic neurons are shown in black, γ-aminobutyric acid (GABA)-ergic fibers in blue, epilepsy-induced changes in red. The loss in parvalbumin (PV)-positive neurons reduces the inhibitory drive on pyramidal cells (39) and may contribute to the seizure development. Axons of calretinin (CR)-immunoreactive (ir) glutamatergic neurons located in the thalamic nucleus reuniens, innervating interneurons, and (to a lesser extent) principal neurons in the subiculum, degenerate after KA-induced SE. Because the fast (8 days after KA) reduction in CR-ir fibers correlates with the frequency of subsequent spontaneous seizures, these events may also be related. Spontaneous seizures developing after KA-induced SE induce pronounced ectopic expression of neuropeptide Y (NPY) in virtually all principal neurons increasing with the number of seizure events. On its release after high-frequency firing (during a spontaneous seizure), NPY may act on presynaptically located Y2 receptors and inhibit further glutamate release terminals of principal neurons. Somatostatin (SOM) is ectopically expressed in pyramidal neurons. In contrast to NPY, this event is observed only 24 hours after KA. Whereas approximately 23% of SOM-ir GABAergic interneurons (homologous to stratum oriens/lacunosum-moleculare and bistratified cells in hippocampal sector CA1) degenerate in the pyramidal cell layer of the subiculum, there is markedly increased SOM-ir in terminals of surviving SOM interneurons in the outer molecular layer (oml) of the subiculum, indicating sprouting in this area. The SOM may support GABA-ergic feedback inhibition on pyramidal neurons through sst2 receptors. Labeling intensity of SOM-ir fibers in the oml of the subiculum correlated with the number of spontaneous seizures and may also be driven by them. **(B)** Increased SOM-ir in the parahippocampal region 3 months after KA-induced seizures. Presumed sprouting of SOM-ir, GABAergic fibers is indicated in the proximal subiculum (rectangle depicts anatomic location of scheme in **A**). **(C)** Ectopic expression of NPY-ir in principal neurons 3 months after SE results in labeling of many important glutamatergic fiber tracts of the parahippocampal region. CA1, hippocampal sector CA1; DG, dentate gyrus; entorhinal cortex (EC) III, entorhinal cortex Layer III; iml and oml, inner and outer molecular layer; PaS, parasubiculum; pcl, pyramidal cell layer; PRC, perirhinal cortex.

Europe PMC Funders Author Manuscripts

Europe PMC Funders Author Manuscripts

TABLE 1

Density of SOM-Immunoreactive Neurons in Parahippocampal Regions of Treated and Control Rats at Different Times After Kainic AcidYInduced Status Epilepticus

Region	KA 24 h (n = 9), %	KA 8 d (n = 9), %	KA 1 mo (n = 10), %	KA 3 mo (n = 15), %
Subiculum	187 ± 9.1*	96 ± 3.7	91 ± 3.4	77 ± 2.7*
Presubiculum	89 ± 7.9	66 ± 5.0†	76 ± 10.8‡	72 ± 5.1†
Parasubiculum	136 ± 15.9†	97 ± 9.0	100 ± 8.4	94 ± 5.4
Entorhinal cortex				
Layers I–II	118 ± 11.7	111 ± 10.8	112 ± 8.7	108 ± 7.2
Layers III–IV	84 ± 6.1	99 ± 7.7	100 ± 7.5	118 ± 6.0
Layers V–VI	100 ± 7.2	66 ± 5.1*	68 ± 3.8*	84 ± 4.0‡

Densities of somatostatin (SOM)-immunoreactive neurons and the respective areas were determined in images of 30-μm-thick sections labeled for SOM using the image processing software ImageJ. Data are presented as percentage of controls (mean ± SEM). The numbers (n) of animals are given in parenthesis; 22 rats were used as controls.

Statistical analysis was performed by analysis of variance with Dunnett multiple comparison post hoc test for group comparisons

*, $p < 0.001$;

†$p < 0.01$;

‡$p < 0.05$.

KA, kainic acid.

Europe PMC Funders Author Manuscripts

J Neuropathol Exp Neurol. Author manuscript; available in PMC 2012 July 18.

TABLE 2

Epilepsy-Induced Changes in the Percentage of Neuropeptide Y mRNA-Expressing Neurons in the Subiculum and Entorhinal Cortex

Region	Controls (n = 9), %	KA 24 h (n = 5), %	KA 8 d (n = 6), %	KA 1 mo (n = 5), %	KA 3 mo (n = 3), %
Proximal subiculum	3.0 ± 0.27	18.5 ± 4.32 * (620 ± 145.0)	11.3 ± 2.07 (379 ± 69.5)	35.7 ± 5.73 † (1198 ± 192.4)	23.9 ± 4.41 * (803 ± 148.2)
Distal subiculum	2.4 ± 0.25	5.6 ± 0.82 (234 ± 33.4)	4.9 ± 0.66 (202 ± 27.5)	9.9 ± 2.09 † (412 ± 86.6)	8.2 ± 0.58 * (340 ± 24.2)
Superficial EC	2.1 ± 0.22	15.0 ± 2.47 † (721 ± 118.5)	6.2 ± 1.67 (297 ± 80.1)	20.2 ± 3.82 † (968 ± 183.1)	15.5 ± 2.31 * (741 ± 110.7)
Deep EC	2.3 ± 0.19	12.6 ± 3.56 † (551 ± 155.9)	6.3 ± 0.79 (274 ± 34.6)	11.1 ± 0.99 † (485 ± 43.8)	7.5 ± 0.16 (327 ± 7.0)

Animal numbers (n) are given in parenthesis. Numbers of NPY-mRNA-expressing neurons were determined in images of 20-μm-thick photoemulsion-dipped sections after in situ hybridization. Data are presented as percent ± SEM. Percent of controls are given in parenthesis.

Statistical analysis was performed by analysis of variance with Dunnett multiple comparison post hoc test for group comparisons

* $p < 0.01$;

† $p < 0.001$.

EC, entorhinal cortex; KA, kainic acid; NPY, neuropeptide Y.

Europe PMC Funders Author Manuscripts

J Neuropathol Exp Neurol. Author manuscript; available in PMC 2012 July 18.

TABLE 3

Time Course of Increases in Neuropeptide Y Immunoreactivity After Kainic Acid–Induced Status Epilepticus

Region	KA 24 h (n = 9), %	KA 8 d (n = 9), %	KA 1 mo (n = 10), %	KA 3 mo (n = 15), %
Proximal subiculum	99 ± 4.2	149 ± 17.8*	193 ± 18.5†	280 ± 28.1†
Distal subiculum	106 ± 5.1	161 ± 27.7‡	169 ± 22.8†	245 ± 24.6†
Presubiculum	88 ± 5.3	108 ± 2.7	99 ± 5.4	140 ± 18.4†
Parasubiculum	91 ± 5.6	123 ± 9.7	152 ± 13.5*	221 ± 52.9†
Medial EC				
Layers II–III	93 ± 3.7	104 ± 3.2	108 ± 5.6	177 ± 30.4†
Layers V–VI	102 ± 6.0	124 ± 8.0*	121 ± 8.1	179 ± 16.9†
Lateral EC				
Layers II–III	129 ± 6.4	153 ± 22.7	248 ± 26.3†	316 ± 55.7†
Layers V–VI	105 ± 5.0	152 ± 17.3*	187 ± 18.3†	264 ± 39.3†
Perirhinal cortex	135 ± 8.5	202 ± 39.2*	322 ± 34.3†	378 ± 64.8†

Relative optical density (ROD) values of neuropeptide Y immunoreactivity (NPY-ir) of the respective areas were determined in images of 30-μm-thick sections labeled for NPY-ir using the image processing software ImageJ. Relative optical densities are presented as percent of controls ± SEM.

Animal numbers (n) are given in parenthesis; 22 rats were used as controls.

Statistical analysis was performed by analysis of variance with Dunnett multiple comparison post hoc test for group comparisons

*$p < 0.05$;

†$p < 0.001$;

‡$p < 0.01$.

EC, entorhinal cortex; KA, kainic acid.